Words: 6,307

Finding a Cure for Malaria Using Chemistry and Social Media

by

Eduvieoghene Omene

The University of Edinburgh
BSc (Hons) Chemistry
17 March 2014

Supervised by: Dr Patrick Thomson and Dr Peter Kirsop

Abstract

Malaria is a life threatening disease which affects millions of individuals worldwide and is caused by the *Plasmodium* parasite. Since its discovery, various antimalarial drugs have been developed to tackle the disease. However, the increasing number of *Plasmodium* parasite species developing resistance to current antimalarial drugs necessitates the development of new, potent antimalarials.

This project was carried out with the aim of synthesising a compound that would be a preclinical candidate antimalarial drug that can then be developed in Phase I trials for treatment of malaria. This target was approached by incorporating the use of Social Media in devising two broad synthetic routes to synthesising a target compound, of which one of these routes was further expanded into three distinct synthetic pathways to the compound. However, by the end of the project, a compound to be tested for potency against the malaria parasite was not successfully synthesised.

Acknowledgements

I would like to thank my supervisors, Dr Patrick Thomson for his wisdom on everything chemistry and Dr Peter Kirsop for his support and guidance.

I would also like to thank Miss Devon Scott for her enthusiasm throughout this project, without which I would not have survived.

Table of Content **Pages**

[1] INTRODUCTION

Malaria is a life-threatening disease caused by the *Plasmodium* parasite, of which the four different species that infect humans are *P. falciparum, P. malariae, P. vivax* and *P. ovale*. The most deadly of these is the *P. falciparum* but all of these parasites need two hosts in order to bring about malaria: a female Anopheles mosquito and a human. [1]

Although treatable, the disease still affects a large number of people, with recent statistics reporting 219 million cases of infected people worldwide, of which 660 000 deaths was estimated, mostly among African children. Together, the Democratic Republic of the Congo and Nigeria account for over 40% of the estimated total of malaria deaths globally.[2] However, with international travel becoming more common, travellers from malaria-free areas are becoming increasingly vulnerable to the disease. [3]

Considering the fact that a large number of individuals are still being affected by this disease, antimalarials have been developed in an attempt to efficiently tackle this problem. The two types of antimalarials available are quinolone- containing antimalarials and artemisinin-based drugs.[4] When treating this disease with antimalarial drugs, recovery from the disease from a parasitological point of view is assessed by the level of parasites that has been cleared from peripheral blood smears. In cases of highly drug-resistant infections, the parasites do not disappear in the peripheral blood, but if they do, their numbers may increase once antimalarial drugs are administered. Contrastingly, in cases of parasites with lower levels of resistance, the parasites disappear from the peripheral

blood but can return at a later time often accompanied with the return of symptoms. Therefore to access how efficiently antimalarial drugs work, it is vital to determine the speed at which symptoms and signs are resolved, the speed at which the levels of parasites in the blood declines and the fraction of individuals who experience reoccurring infections within a defined period.[5] Considering all these factors, artemisinin based drugs prove to be the most effective antimalarial for malaria treatment today, but the development of resistance of the most dangerous malaria parasite strain, i.e. *P. falciparum* to artemisinin provides an incentive for new antimalarials to be developed. [4]

To successfully develop a potent antimalarial drug, it is important to not only understand the life cycle of the *Plasmodium* parasite but also gain knowledge of how current antimalarials work in the body.

[1.1] *Plasmodium* Parasite and Antimalarial drugs

Figure 1 illustrates the life cycle of the *Plasmodium* parasite. It begins when an infected female mosquito bites her human prey, withdrawing blood and injecting sporozoite-containing saliva into the humans skin capillaries.

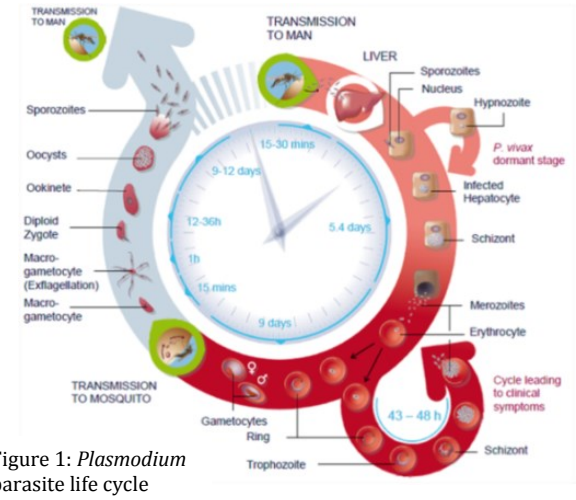

Figure 1: *Plasmodium* parasite life cycle

The sporozoites then enter liver cells

and multiply to form about 30,000 merozoites each, which get released into the blood stream where they enter red blood cells i.e. erythrocytes and develop through the schizont stages.

Whilst in the erythrocyte, the parasites go into the trophozite stage whereby they grow and multiply by ingesting hemoglobin, which propels the production of 16–20 daughter merozoites that burst from the erythrocyte to invade new red blood cells and restart the cycle. It is this intraerythrocytic stage of the malaria parasite that produces the disease pathology. After several cycles, some of the intraerythrocytic parasites develop into sexual stage gametocytes. The gametes are ingested when a mosquito bites an infected individual. They mate in the gut of the insect and then pass through the gut wall, where they develop into oocysts which release sporozoites that migrate to the salivary glands to be passed on to another individual.[6]

In summary, the malaria parasite differentiates into a series of morphologically distinct forms in the vertebrate and mosquito hosts. It alternates between invasive stages (sporozoite, merozoite, and ookinete) and replicative stages (pre-erythrocytic, erythrocytic-schizont, and oocyst) interpolated by a sexual development phase that mediates transmission from the human host to the Anopheline vector. [7]

In the treatment of malaria, although certain antimalarial drugs may be very potent, none of them act instantaneously, even if the drug is administered intravenously. Interestingly, the level of parasites in the blood increases in the first few hours following the administration of the drug, particularly in cases

where the patient is being treated at a time when the parasites have entered the erythrocytes and are developing through the schizonts stage, because as these erythrocytes rupture they release merozoites which invade and infect circulating uninfected erythrocytes. Malaria caused by the *P. falciparum* parasite may also exhibit a decline in the level of parasites in the blood immediately following treatment because of a build-up of an infection happening at the same time. In these cases, the majority of parasites in the peripheral blood are in the early trophozoites stage which is where antimalarial drugs are most active. Determining how effective the drugs work is achieved by monitoring how efficiently the drug inhibits the uptake of glucose, amino acids, and purine. Most of the available antimalarial drugs achieve this by inhibiting the parasites trophozoite stage of development which causes a considerable reduction in the parasite multiplication rate. Considering that the activity of antimalarials is most effective at this particular stage of the parasite development, the timing of drug administration with respect to the stage of parasite development also plays a role in determining the therapeutic response in the patient. [5]

With this information at hand, pharmaceutical companies strategically synthesise antimalarials by mainly using traditional methods of drug discovery. However, this project utilised a less conventional method of drug synthesis by incorporating the use of Social Media.

[1.2] Social Media in synthesis of Antimalarials

This project was aimed at synthesising a potent antimalarial drug by working in conjunction with the Open Source Malaria (OSM) team. The OSM team utilise a non-traditional means of drug discovery, as all research is reported openly and online, through Social Media platforms such as Twitter, Facebook and GitHub. This allows scientists from around the globe to collaborate together in strategising and synthesising various compounds for testing against malaria. The experimental procedures carried out by members of the team for each synthesised compound is documented in publicly accessible online notebooks, along with the raw data from analysis of the compounds. This not only allows for feedback from other team members on particular synthetic routes, but in this particular project, it allowed for experimental results to be compared with the raw data documented by others. This was particularly useful when compounds which do not have analytical data published in literature were synthesised, as the data derived for such compounds could be compared to the raw data documented by other members of the team. Results are also discussed between the group members via well-organised online meetings which encourages the strategic developments of new synthetic routes when necessary and facilitates the progress of ongoing synthetic pathways.

Prior to joining the OSM team, the Series 4 triazolopyrazine compound was being worked on by other members of the team, of which the representative compound, **1** in the series is shown in Figure 2. [8]

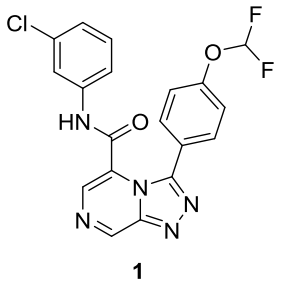

1

Figure 2: Representative compound of the OSM triazolopyrazine series

The Malaria for Medicine Venture (MMV) had placed this compound in the public domain, thus allowing access to companies, individuals and organisations who are interested in investigating its potency. The OSM team discovered that in the treatment of malaria, compound **1** has particularly high potency and in vivo efficacy with few toxicity concerns. Particular interest in the compound developed when experimental testing revealed a possible *Plasmodium falciparum* calcium (II) -ATPase (PfATP4) activity.[8] This is because the PfATP4 proteins are vital components of the machinery used by eukaryotic cells to regulate intracellular calcium concentrations. Moreover, the PfATP4 defines a novel subclass of calcium (II) -ATPases, thus providing a unique category for potential drug target. As the *Plasmodium falciparum* parasite belongs to a class of organisms known as apicomplexan organisms, they require transport proteins such as PfATP4 in order to grow and replicative,[9] so targeting these proteins is a good strategy for making new antimalarials. The main issue with compound **1** was discovered to be its metabolic instability[8], so the direction of this project was to synthesise derivatives of the compound **1**, which contain structural modifications that would hopefully improve its potency and metabolic stability.

As highlighted previously, some of the factors that affect the efficiency of antimalarial drugs are its ability to interact with the erythrocytes, their inhibitory effects on certain nutrients such as glucose, and the stage of parasite development at which the drug is administered.[5] By targeting the phenyl ether side chain on the pyrazine ring of **1**, the OSM team was able to determine that it was a metabolic hot spot, which upon modification to introduce other functional groups, affected the potency of the compound. They found that changing the length of the side chain to anything more than three atoms severely lowered the potency of the compound.[8] This could be because having a bigger side chain lowers the compounds ability to inhibit the uptake of those nutrients needed for growth. It was also noted that the linker atom to the pyrazine ring is also very crucial as reflected in Figure 3, whereby compound **2** which has oxygen as the linker atom is reported to be fifteen times more potent than compound **3** that has nitrogen as the linker atom [8]

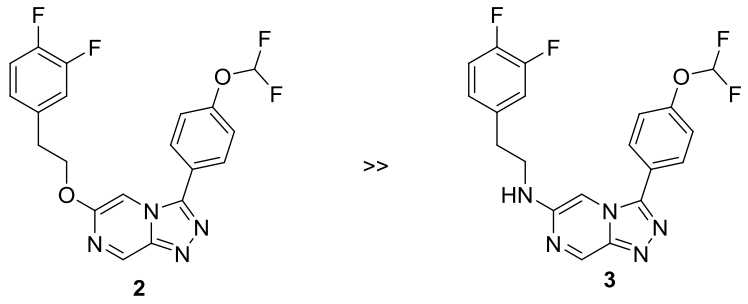

Figure 3: Potency comparison between triazolopyrazine compounds with different linker atoms

Oxygen, being more electronegative than nitrogen might interact with electron rich species in the body, which might increase the ability for **2** to inhibit the uptake of glucose or other nutrients, therefore making it more potent than **3**. It

was also noted that having heteroatoms within the side chain lowered the potency,[8] which could be as a result of reduced interaction with the erythrocytes. Considering these factors, the target compound **4** as shown in in Figure 4 was designed, and the main focus of the project was attempting to synthesise this compound.

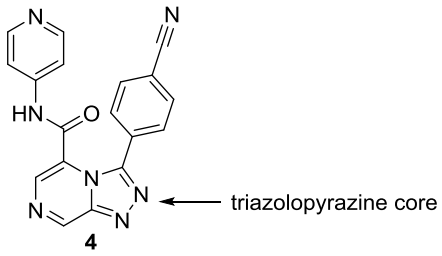

Figure 4: Target compound for synthesis

[2] RESULTS AND DISCUSSION

In all the compounds of the triazolopyrazine series that were synthesised by members of the OSM team, a common thread which was evident in all of the compounds that displayed high levels of potency was the presence of the triazolopyrazine core[8], which is also present in the target compound **4**. Thus a good starting point for this project was focused on synthesising this core, upon which the side chain substituents would then be added. However attempts at this synthesis highlighted some challenges, which warranted the need to develop other synthetic routes to compound **4**. Therefore the second part of this project focused on synthesising compound **4** via the synthesis of the substituted pyrazine ring which would then be cyclised to give the triazolopyrazine core with the needed side chain atoms already present.

[2.1] Synthesis of the triazolopyrazine core

Scheme 1 outlines the synthetic route to generating the triazolopyrazine core.

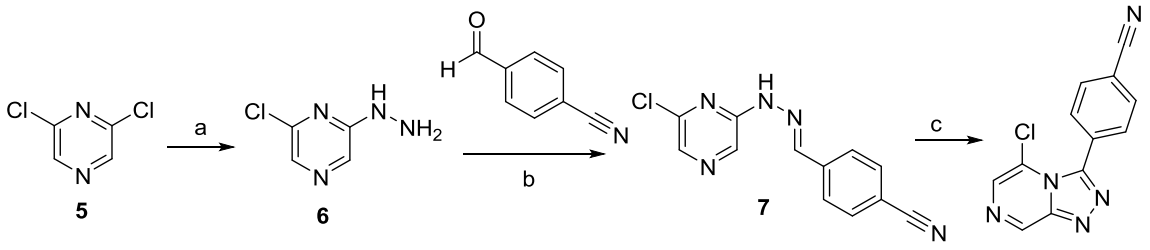

Scheme 1: Synthetic scheme for triazolopyrazine core. a.)EtOH, NH_2NH_2, 105 ^oC, 16 h, 78%; b.)MeCN, AcOH, rt, 2 h, 75%; c.) $PhI(OAc)_2$, CH_2Cl_2, rt, 25 h, 14%.

The first part of the triazolopyrazine core synthesis relies on a nucleophilic substitution reaction whereby hydrazine acts as a nucleophile that attacks the halide carbon in 2,6–dichloropyrazine, **5** to yield 2-chloro-6-hydrazinylpyrazine, **6**. Evidence that this reaction had worked was shown in the ^{1}H NMR data derived which matched the literature data[10] and the melting point determined (130-132^{o}C) which was close to the melting point recorded in literature (136-139 ^{o}C) [10] Subsequent condensation of **6** with 4-formylbenzonitrile produced compound **7** which was then cyclised using phenyliodinediacetate (PIDA) via an oxidative cyclisation reaction. This oxidative cyclisation step proved to be the lowest yielding step (14 %) and the mechanism which is based on literature[11] is shown in Scheme 2

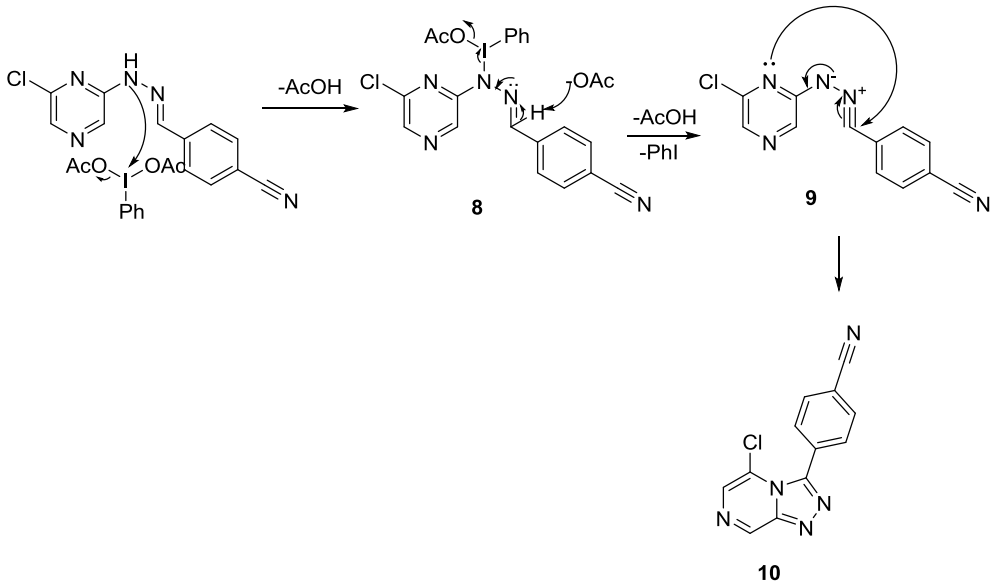

Scheme 2: Mechanism for oxidative cyclisation using PIDA

The intermediate **8** is formed from the reaction of **7** with PIDA by losing one molecule of acetic acid. Subsequent de-protonation, loss of another acetic acid molecule and loss of phenyliodine forms the intermediate **9** which then

undergoes electrocyclic ring closure to afford the cyclised product **10** which was then characterised by NMR analysis.

Analytical data containing ^{1}H NMR information on compound **10** is not available in literature. However, comparing the ^{1}H NMR derived, with the ^{1}H NMR reported by members of the OSM team[12] provided some evidence to suggest that **10** had formed as both spectra were very similar. However, the extremely low yielding cyclisation step proved to be the problematic part of this synthetic attempt. The low yield could be because the cyclisation process involves the formation of a five-membered ring which contains three electron rich nitrogen atoms in close proximity to each other. Therefore the level of electron-electron repulsion would be high, which would make the reaction less favoured. Thus it was crucial to determine reaction conditions which would facilitate a potential increase in the yield by making the formation of the cyclised product more favourable. Indeed, other reported cyclisation reactions involving the use of PIDA highlighted that the yield of cyclised product is highly dependent on the reaction conditions employed. In the synthesis of indole compounds for example, the yield of product has been shown to vary from 61 % to 84 % and the most optimised conditions which gave the highest yield was determined to be when the reaction was carried out at 60 ^{o}C for 2 hours and with 1.3 equivalents of PIDA. Deviating from these optimised conditions, either by raising the temperature or raising the amount of PIDA used, caused a decrease in yield[11] thus highlighting the sensitivity of the cyclisation reaction to these factors. The reaction conditions used in this reaction could be the determining factor that affected the yield of cyclised product **10**. Therefore, adjusting the conditions used in this experiment,

whilst monitoring the yield of product could be a strategy employed to optimise the amount of product produced.

[2.2] Synthesis of pyrazine ring with side chain substituents

Having discovered the need to optimise the oxidative cyclisation step when synthesising the triazolopyrazine core, the focus of this project shifted towards synthesis of compound **4** via the formation of a substituted pyrazine ring, after which applications of the optimal PIDA cyclisation conditions or other cyclisation reactions would be employed to give the final product. Attempted synthesis of compound **4** via this strategy led to the development of three distinct synthetic routes. However by the end of the project, a compound to be tested for antimalarial activity was not successfully synthesised.

The retrosynthetic scheme for compound **4** is shown in Scheme 3

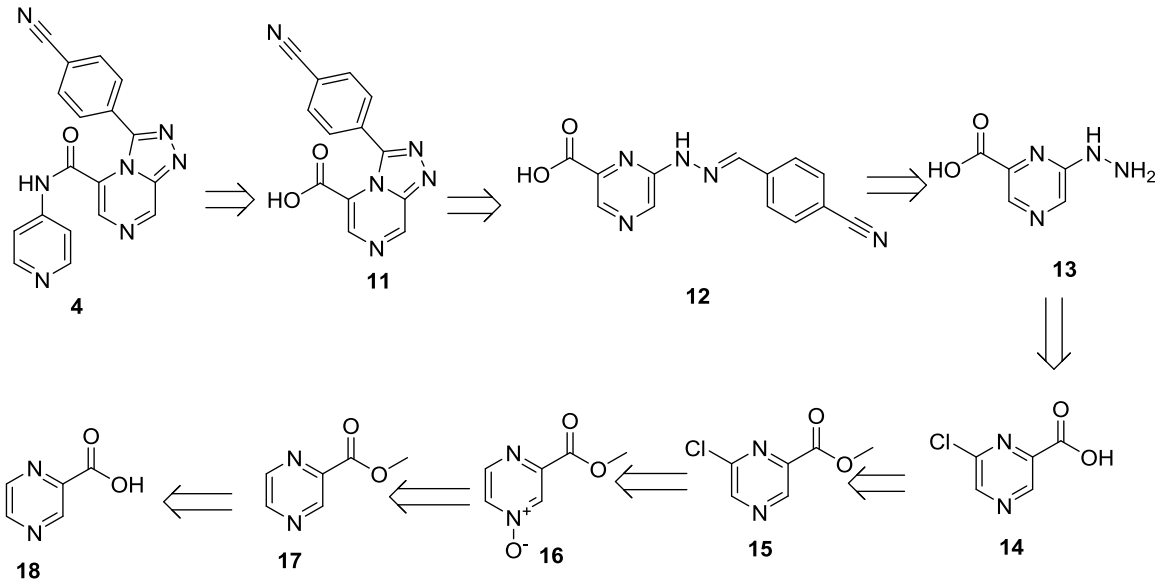

Scheme 3: Retrosynthetic scheme for compound **4**

In order to produce **4**, a condensation reaction between **11** and 4-aminopyridine can be carried out. Breaking the five-membered ring in **11** will give compound **12** which can be used to generate **11** via an oxidative cyclisation reaction, but can also be produced via another condensation reaction between **13** and 4-formylbenzonitrile. In turn, **13** can be produced through a nucleophilic substitution reaction between **14** and hydrazine, whilst **14** can be generated via hydrolysis of the ester in **15**. Selective chlorination of **16** using thionyl chloride gives **15** whilst **16** can be formed through the oxidation of **17** using *meta*-chloroperoxybenzoicacid *(m*CPBA). In turn **17** can be produced via esterification of the readily available starting material, pyrazine-2-carboxylic acid, **18**.

[2.2.1] First Synthetic attempt

The first synthetic attempt at producing **4** relied on carrying out the reactions described above, as shown in Scheme 4

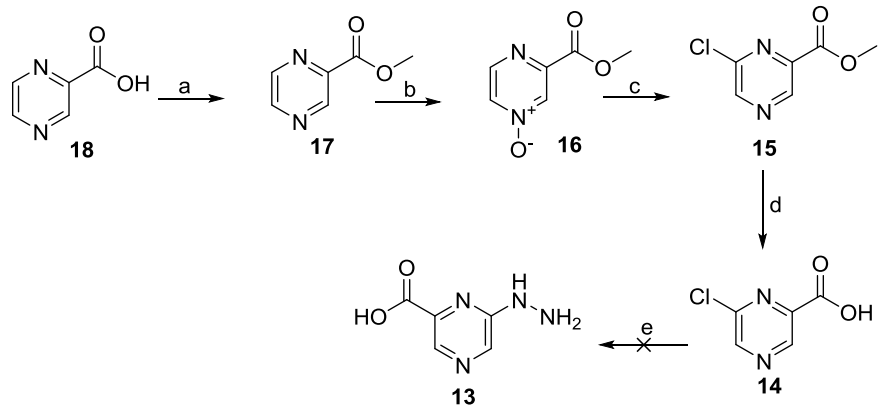

Scheme 4: Synthetic scheme for first attempt at synthesising compound **4** a) H_2SO_4, MeOH, reflux, 48 h, 84%; b) *m*CPBA, DCE, 60 ^oC, 16 h, 54%; c) $SOCl_2$, reflux, 8 h, 22% d) NaOH, EtOH, rt, 2 h, 49%; e) NH_2NH_2, EtOH, reflux, 16 h.

The first step was a straightforward esterification reaction of pyrazine-2-carboxylic acid, **18** to produce methylpyrazine-2-carboxylate, **17** which ^{1}H NMR confirmed had indeed been made, as it matched published literature ^{1}H NMR data.[13] The next step which produces the *N*-oxide, **16** involved the activation of the nitrogen atom in **17** with an electron rich oxygen. This was a crucial step that is needed to facilitate the selective chlorination of **17** to give compound **15**. Normally, aromatic compounds are chlorinated via electrophilic aromatic substitution reactions using the polarised chlorine ($Cl^{\delta+}$) as the electrophile, but in the case of pyrazine this reaction cannot happen because the nitrogen atoms end up reacting with the electrophile. This explains why it was necessary to activate compound **17**. This activation was done by using a strong oxidising agent, *m*CPBA which oxidises the nitrogen in **17** to the highly activated *N*-oxide compound, **16**.

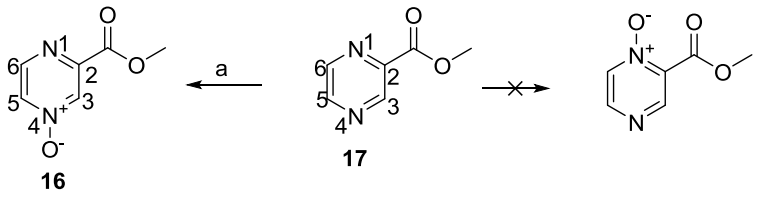

Scheme 5: Possible oxidation routes for **17.** a) *m*CPBA, DCE, 60 ^{o}C, 16 h, 54%.

From the structure of **17** as shown in Scheme 5, it is clear to see that there are two nitrogen atoms, N-1 and N-4 which can be oxidised. However, it has been shown that the oxidation of this particular carboxylate exclusively proceeds at the N-4 nitrogen to form methyl 4-oxy-2-pyrazinecarboxylate, **16** [14] Therefore in this experiment, it was expected that oxidation should only occur at the 4 position. When this oxidation reaction was carried out, it was initially carried out

on a fraction of the carboxylate, **17** so as to determine if the desired *N*-oxide had formed. The ^{1}H NMR analysis of the resultant solid matched that which is recorded in literature [15] which provided evidence to suggest that the N-4 nitrogen had indeed been the nitrogen that was oxidised. Nonetheless, the ^{1}H NMR spectrum also showed the presence of peaks which correspond to *m*CPBA that had not reacted and was still present in the solid. Therefore, a small-scale purification was carried out on the solid using ethyl acetate, sodium bicarbonate and brine which removed the desired *N*-oxide **16** from the aqueous layer into the organic layer, whilst *m*CPBA remained in the aqueous layer. Another ^{1}H NMR spectra of the resultant solid from the organic layer was derived, which showed that *m*CPBA had successfully been removed. Therefore, the same purification process was carried out on larger scale using the rest of the impure *N*-oxide **16.** Table 1 shows the yields of the *N*-oxide **16** after the purification process

Scale	Percentage yield/ %
Small scale purification	53
Large scale purification	3
Large scale purification and re-extraction	54

Table 1: Percentage yields after purification processes of **16** on different scales

Although the purification procedure carried out was exactly the same, Table 1 shows that there was a dramatic decrease in the yield of product when carried out on a larger scale. This is because the *N*-oxide product **16** was very soluble in water so most of it remained in the aqueous layer. Taking this into account, the remainder of the carboxylate **17** which had not been oxidised was reacted with *m*CPBA, but this time an extraction procedure was added. After the purification

of the oxidised solid was carried out using ethyl acetate and sodium bicarbonate, a sample of the aqueous layer solution was used for TLC analysis against the product from the previous low yielding oxidation and purification process. The TLC indeed indicated that there was still product in the aqueous layer, therefore an extraction of product from this layer was carried out by three consecutive additions of specific amounts of dichloromethane and methanol. TLC of the final aqueous layer showed that the entire product had been extracted into the organic layer, which went on to produce the pure solid product **16** in 54 % yield. The ^{1}H NMR and melting point derived (108 ^{o}C) matched the ^{1}H NMR and melting point (110–112 ^{o}C) data reported in literature[15] which provided evidence to show that **16** had successfully been synthesised.

The next step of this synthetic attempt was the chlorination of the *N*-oxide, **16**. Pyrazine *N*-oxides with substituents at the 2 position can be halogenated predominantly at the C-3 and C-6 carbons as shown in **16**. The delocalisation of the electrons on the oxygen around the pyrazine ring raises the energy of Highest Occupied Molecular Orbital (HOMO) and allows for useful nucleophilic substitution reactions to take place[16] which is the mechanism that produces one of the possible halogenated compounds, **19**. In addition, if the substituent on the pyrazine *N*-oxide is an electron-withdrawing group, then the product would predominantly be the 6-halide, **15** whereas if the substituent is an electron-donating group, then the 3-halide **19** would be the major product. Therefore the expected product upon chlorination of **16** was **15**. Scheme 6 highlights the mechanisms that would generate the two chlorinated products **15** and **19**, of which mechanism 2 that yields **15** was derived from literature [14]

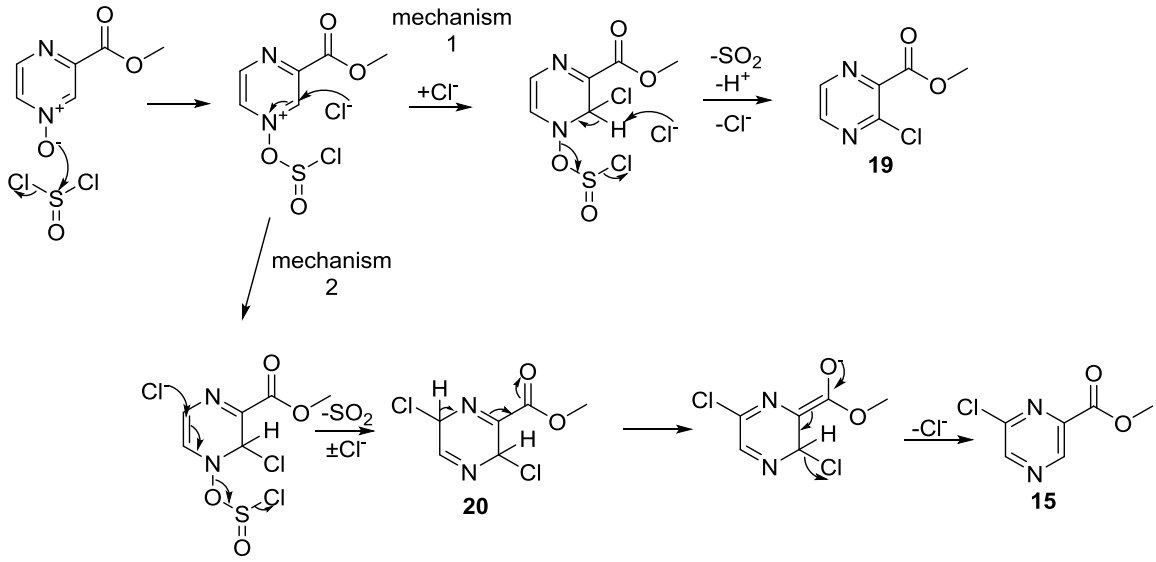

Scheme 6: Competing mechanism for chlorination of activated *N*-oxide, **16**

For both mechanisms, the first step is the reaction of the *N*-oxide with thionyl chloride through oxygen whereby the chloride ion released adds onto the ring, through a nucleophilic substitution reaction which is encouraged by having a positive nitrogen. The chlorine selectively adds onto the carbon which is *ortho* to the positive nitrogen of the *N*-oxide as this is the most electrophilic position. In mechanism one, a simple elimination restores aromaticity and produces **19** looking as though it resulted from chlorination as opposed to nucleophilic substitution[16]. In mechanism two, nucleophilic attack by another chloride ion and desulfurisation produces the intermediate **20** which was then led to produce **15** simply by mesomeric effect of the carbomethoxy group.[14]

When this reaction was carried out, TLC analysis was done on the resultant oil using five percent ethyl acetate in dichloromethane. Interestingly, three separate spots were observed on the TLC plate, with Rf values of 0.114 cm, 0.57 cm and

0.74 cm. This implied that the oil did not just contain the desired compound **15**, but other compounds were present as well, of which one possible compound could be the 3-halide, **19.** Therefore, the two possible compounds which could be present in the oil are **19** and **15** as shown in Scheme 7.

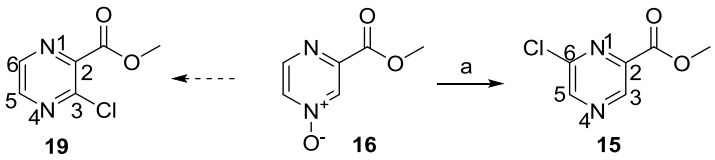

Scheme 7: Possible products from chlorination of **16.** a) $SOCl_2$, reflux, 8 h.

By utilising ^{1}H NMR analysis, it is possible to distinguish between compound **19** and compound **15** as the aromatic H-5 and H-6 protons in **19** are expected to give doublet peaks whereas the aromatic H-3 and H-5 in **15** are expected to give singlet peaks. The ^{1}H NMR of the oil produced is shown in Figure 5

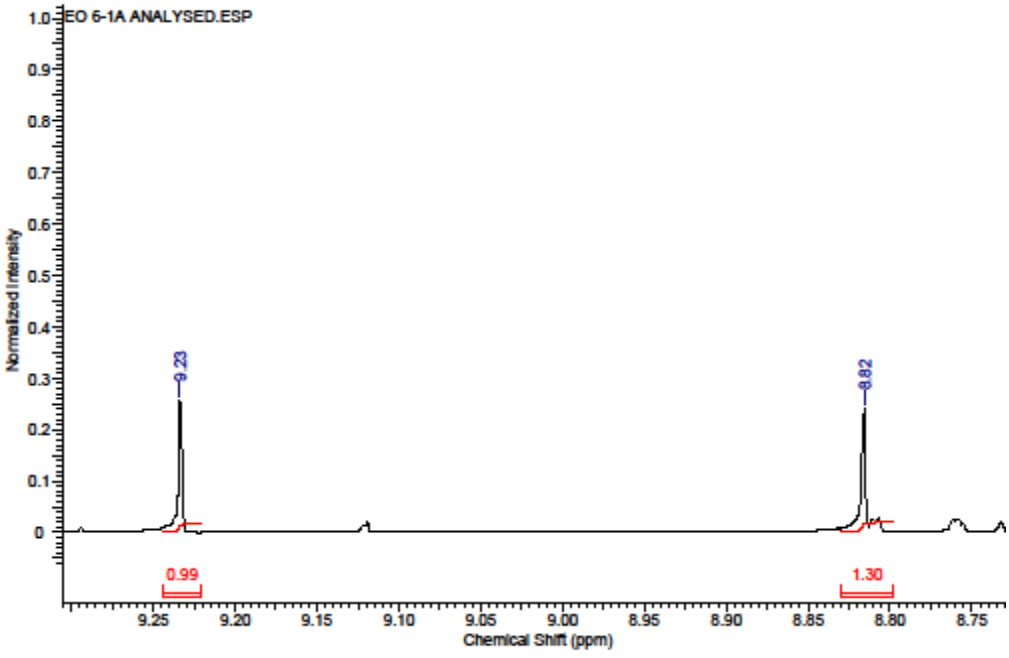

Figure 5: ^{1}H NMR of impure oil of compound **15**

The singlet peaks at 8.82 ppm and 9.25 ppm in a 1:1 ratio correspond to H-3 and H-5 in compound **15** which showed that the oil predominantly contained the desired compound **15**. However, the oil was still purified using flash chromatography to isolate and remove the undesired compounds that TLC had shown to be present.

The resultant solid from the first eluted solution produced an Rf value of 0.594 cm upon TLC analysis and the ^{1}H NMR spectrum derived is shown in Figure 6.

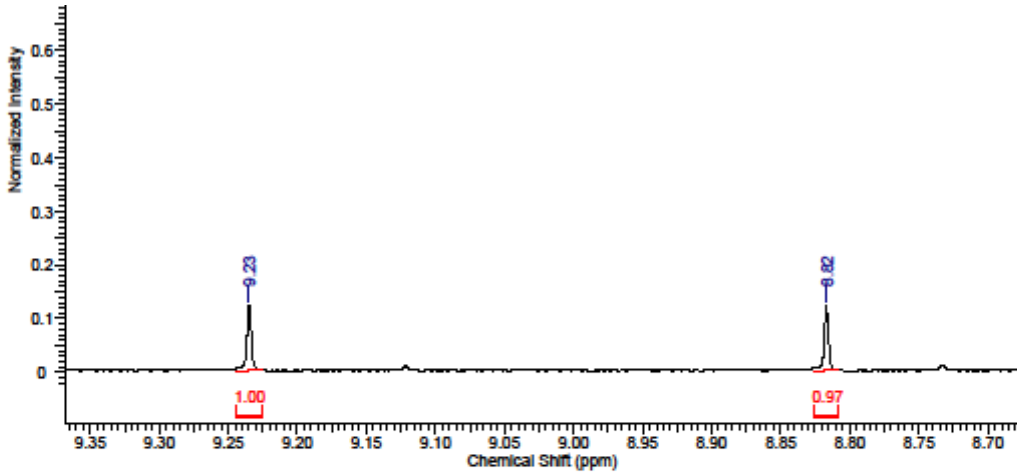

Figure 6: ^{1}H NMR from first eluted sample

This spectrum indicated that the solid contained the desired product as the singlet peaks at 8.82 ppm and 9.23 ppm with a 1:1 ratio correspond to H-3 and H-5 protons in compound **15**. The melting point of the solid derived (40-43 ^{o}C) was the same as the literature melting point of the desired compound **15** (41–44.5 ^{o}C)[14] which provided additional evidence to suggest that the solid formed was the desired compound, **15**.

The resultant solid from the second eluted solution produced an Rf value of 0.586 cm upon TLC analysis but the ^{1}H NMR data did not show any of the significant product peaks at approximately 9.2 ppm and 8.8 ppm. The melting point which was derived (65 ^{o}C) was also significantly different from the literature melting point[14] of the desired compound **15**, so the sample was discarded.

The resultant solid from the third eluted solution produced an Rf value of 0.125 cm upon TLC analysis and the ^{1}H NMR spectrum derived is shown in Figure 7.

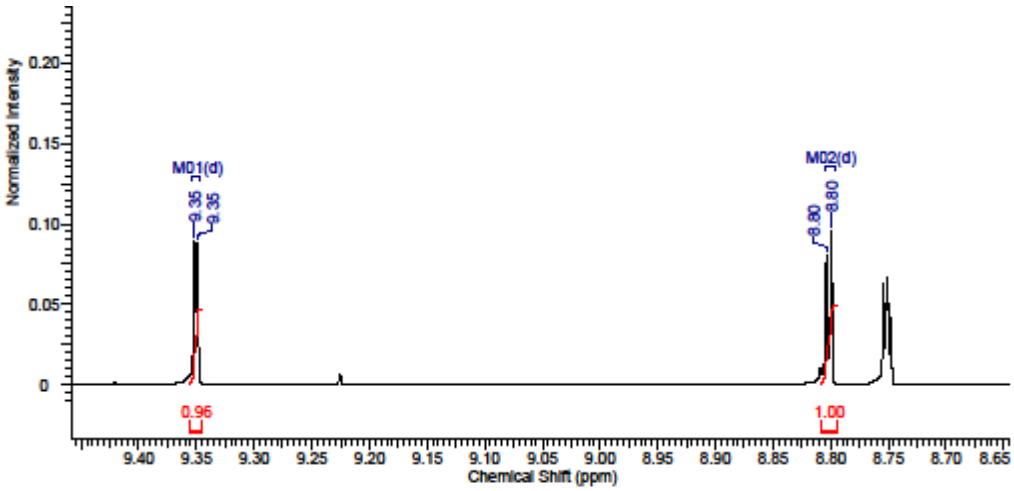

Figure 7: ^{1}H NMR from third eluted sample

This spectrum showed that the solid contained the undesired product **19** as reflected in the doublet peaks observed at 9.35 ppm and 8.80 ppm in a 1:1 ratio which corresponds to H-5 and H-6 protons in compound **19**. The melting point which was derived (35 ^{o}C) was also significantly different from the literature melting point of the desired compound **15**[14], so the sample was discarded.

Using this information, the solid from the first eluted solution which contained the desired compound **15** was taken on to the next step which was the hydrolysis of the ester in **15** to give compound **14.** Mass spectrometry data taken of the resultant solid of this reaction provided evidence to show that the reaction had worked as the peak at 157.9 m/z which represents the molecular ion of compound **14** was observed. ^{1}H NMR of the solid also matched literature data [17] which provided supporting evidence of a successful reaction.

Reacting **14** with hydrazine was the problematic part of this synthesis. The reaction between the two compounds is a straightforward condensation reaction through nucleophilic acyl substitution whereby the desired mono substituted hydrazine product **13** is produced when hydrazine displaces the chlorine atom in **14.** However, prior to carrying out the experiment, the possibility of the hydrazine displacing the hydroxyl group on the carboxylic acid in **14** to generate the undesired hydrazide **21** as shown in Scheme 8 was not explored. Nevertheless, mass spectrometry data of the solid produced after the reaction which is shown in Figure 8 showed that the undesired hydrazide **21** had formed, as the peak at 169.0 m/z is equivalent to the protonated hydrazide product **22.**

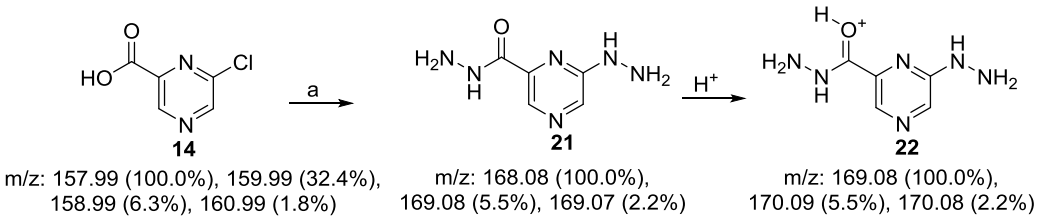

Scheme 8: Generation of double hydrazide compound. a) NH_2NH_2, EtOH, reflux, 16 h.

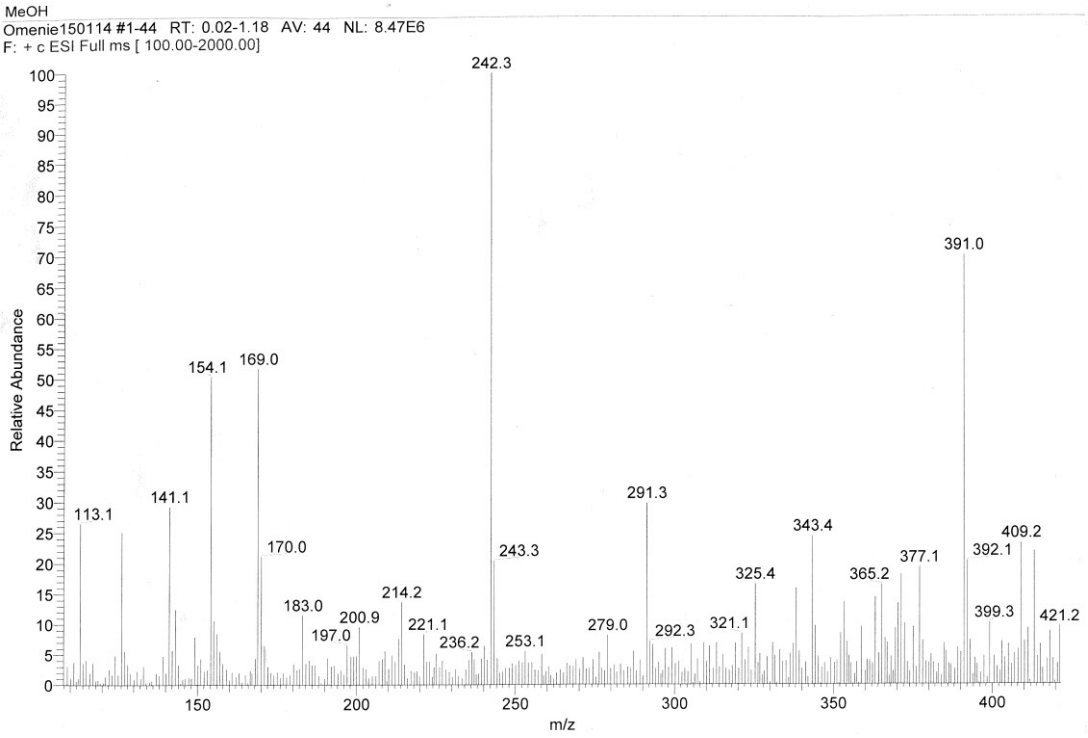

Figure 8: Mass Spectrum of **22**

A possible reason as to why this occurs lies in understanding the electronic structure of pyrazine.

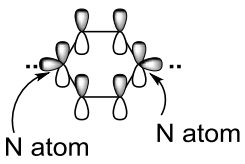

Figure 9: Orthogonal orbitals in pyrazine

Figure 9 shows that the lone pair of electrons on the nitrogen atoms are in an sp^2 orbital which is orthogonal to the p orbitals in the ring. This means that the lone pair of electrons on the nitrogen atoms cannot be delocalised around the ring because there is no interaction between orthogonal orbitals. Therefore the electron density around the nitrogen is very high. In turn, having the highly electronegative nitrogen atoms with a high electron density around it lowers the energy of all the orbitals, including the p-orbitals of the aromatic ring. This means that both the filled orbitals and the unoccupied orbitals in the ring are of lower energy. Having filled orbitals which are lower in energy makes the aromatic ring a less reactive nucleophile, whereas having the Lowest Unoccupied Molecular Orbital (LUMO) with lower energy means that the ring is a more reactive electrophile[18]. This means that the nitrogen atoms make pyrazine more reactive towards nucleophilic substitution which could be a contributing factor as to why the hydrazine reacts with **14** to form the hydrazide **21**.

[2.2.2] Second synthetic attempt

As highlighted above, from the first attempt at synthesising **4**, it was discovered that the carboxylic acid group in **14** was susceptible to reacting with hydrazine to form **21**. Therefore, in order to prevent the carboxylic acid component from reacting, an amide coupling reaction between **14** and 4-aminopyridine was carried out using the carbodiimide, 1-ethyl-3-(3-dimethylaminopropyl) [EDC] to form the amide **23**. Once the amide had formed, the carboxylic acid component was subsequently blocked from reacting with hydrazine. After the coupling

reaction was carried out, the resultant solid was then reacted with hydrazine, thus allowing the hydrazine to displace the chlorine atom as shown in Scheme 9

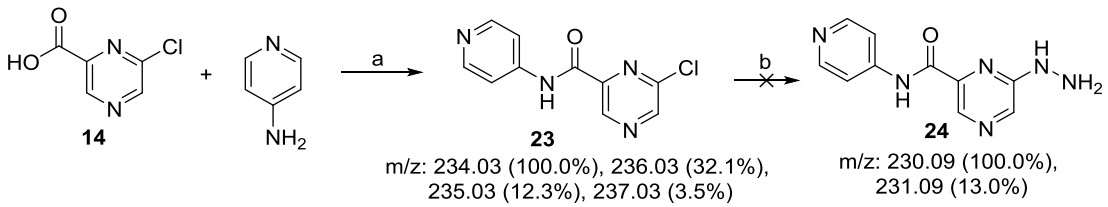

Scheme 9: Reaction scheme of second synthetic attempt of **4** a) DMF, EDC-HCl, HOBt, DIPEA, rt, 16 h, 25%. b) NH_2NH_2, EtOH, reflux, 60 h

When this coupling reaction was carried out, the resultant solid was characterised using mass spectrometry and ^1H NMR analysis. For this reaction in particular, it was crucial to carry out mass spectrometry analysis of the solid because of the different side products that can form when carbodiimides are used in amide synthesis. Although carbodiimides are effective at facilitating the formation of amide bonds, when they are used for this purpose, there are a number of competing pathways that can take place, which yield both the desired product and undesired by-products as highlighted in Scheme 10.

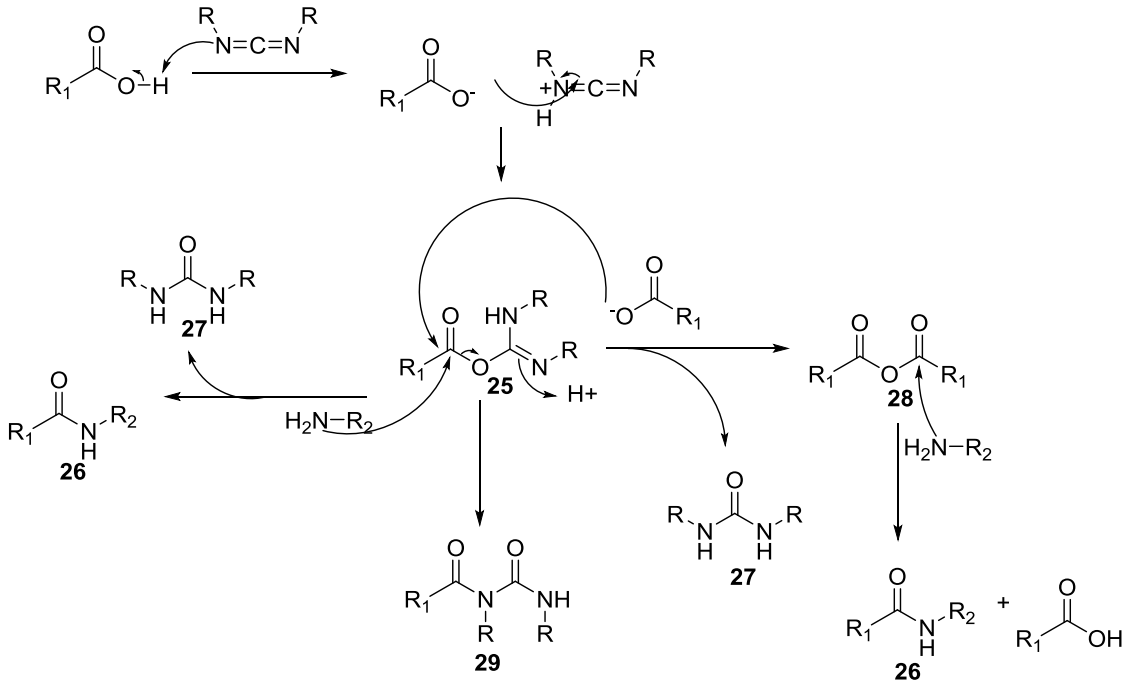

Scheme 10: Competing mechanisms in amide synthesis

As evident in Scheme 10, the *O*-acylisourea, **25** is the key intermediate compound because it can react in a number of ways. It could react directly with the amine to give the amide **26** and urea **27** or it can react with another carboxylic acid to give the symmetric acid anhydride **28** which in turn can react with the amine to give the desired amide **26**. The main undesired pathway which **25** could take would be the intramolecular oxygen-nitrogen shift to give the stable *N*-acylurea compound **29** which cannot be used to generate the amide.

To reduce the level of side reactions that could occur in this reaction, a nucleophilic coupling additive, 1-hydroxy-1,2,3-benzotriazole (HOBt) which suppresses the *N*-acylurea **29** formation was added. Scheme 11 shows how this works.

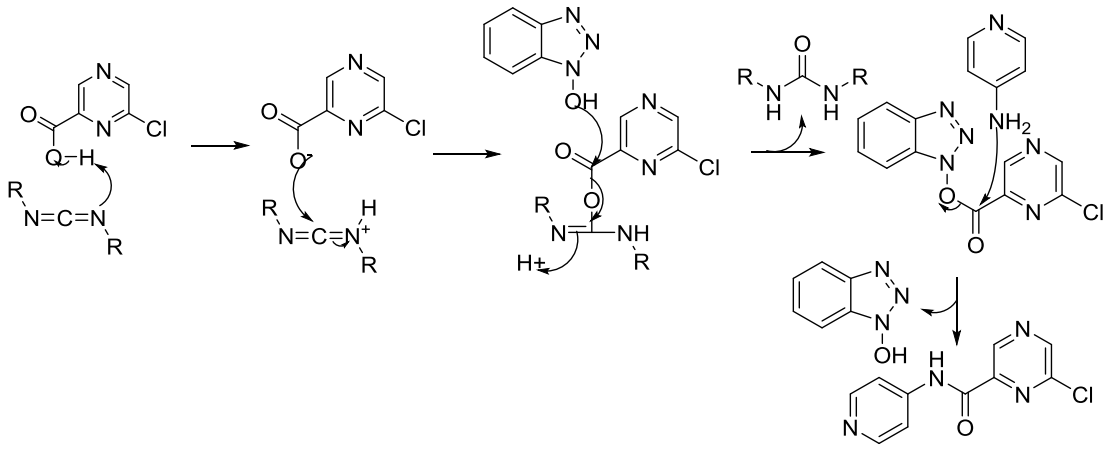

Scheme 11: Mechanism for amide synthesis using HOBt. R = CH_2CH_3 R_1 = $CH_2CH_2CH_2N(CH_3)_2$

The *O*-acylisourea intermediate **25** reacts readily with HOBt to form an activated ester which is non –isolable. However the active ester is less reactive than the *O*-acylisourea intermediate so less likely to undergo side reactions. Most importantly, it can still be attacked by the amine but cannot undergo the intramolecular shift that yields the *N*-acylurea, **29**. This mechanism highlights that the choice of base is also important in this amide coupling reaction because nucleophilic bases could react with the activated ester instead of the amine. Therefore, the tertiary amine, N,N-Diisopropylethylamine (DIPEA) was used, due to its non-nucleophilic property [19]

Unfortunately, even with the use of the additive, mass spectrometry data of the resultant solid confirmed that side reactions had still occurred and urea had formed, as a peak at 174.2 m/z which corresponds to the urea compound **30** as shown in Figure 10 was observed.

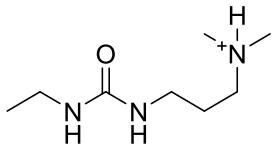

30

m/z: 174.16 (100.0%), 175.16 (9.8%)

Figure 10: Urea by-product from EDC coupling reaction

Product peaks at 234.0 m/z were not present in the spectrum as it predominantly showed the urea peak. Therefore, an acid work-up was carried out on the solid using hydrochloric acid, which eliminates urea, after which another mass spectrum was obtained as shown in Figure 11

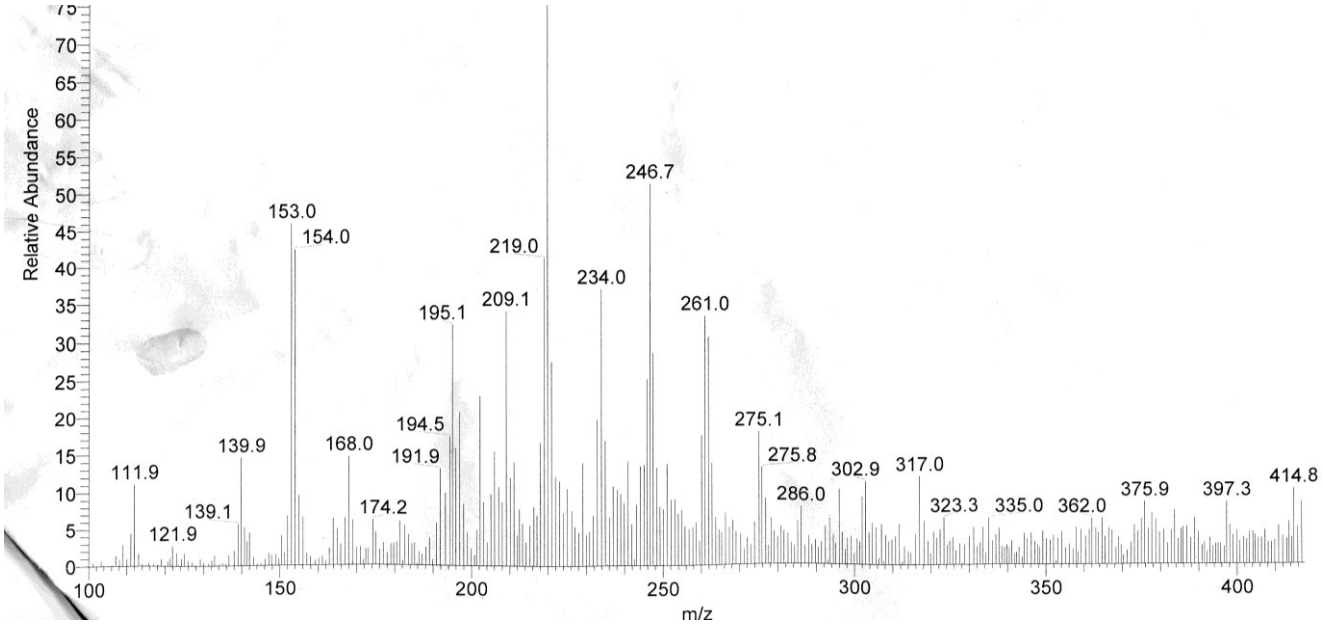

Figure 11: Mass spectrum of **23**

This time the product peak was observed at 234 m/z and the urea peak at 174.2 m/z was significantly smaller. This provided evidence to show that compound **23** had successfully been formed. Additional evidence to support this was

derived from the ^{1}H NMR data which showed the amide proton singlet peak at 7.9543 ppm.

Although this reaction had worked, the yield of product was very low (25 %). This can be improved by employing other technique used in amide coupling reactions, such as attaching compound **14** on a hydrogel before the reaction is carried out. That way, it is possible to separate and analyse the reaction products at any time during the reaction just by removing the gel from the reaction batch[20] thus allowing the reaction to be monitored as it occurs so as to identify the specific procedure that is low yielding. An alternative application of EDC which might effectively increase the yield would be attaching the EDC compound to a polymer to give the polymer bound EDC (PEDC). PEDC behaves similarly to EDC, but the advantage is that the by-products of the reaction would remain on the polymer. Therefore, the product can be isolated simply by filtration and evaporation of the filtrate.[21] Another adjustment that could improve the yield would be using another coupling additive, specifically, 1-hydroxy-7-aza-benzotriazole (HOAt) because HOAt has been reported to be more efficient than HOBt due to its pyridine ring which causes an anchimeric assistance effect [19]

To complete this synthetic attempt, a nucleophilic substitution reaction using hydrazine was carried out on the amide product **23**, as shown in Scheme 9, thus allowing the hydrazine to displace the chlorine atom. A standard work up involving the use of hydrochloric acid, ethyl acetate and lithium chloride was carried out to remove urea and dimethylformamide, upon which the resulting solid was characterised. Mass spectrometry revealed that the reaction had not

worked as the crucial peak at 230.09 m/z which represents the molecular ion of the hydrazine product **24** was not observed.

A reason for the unsuccessful reaction could be due to the presence of other compounds in the solid as evident in the mass spectrum shown in Figure 11 which shows a variety of peaks. As discovered in the first synthetic attempt, where hydrazine reacted with **14** in an unpredictable manner to form the hydrazide, **21**, it could be that the other unidentified compounds in the solid could equally have reacted with hydrazine in a manner which is unprecedented but perhaps more energetically favourable than the reaction between hydrazine and **23** would have been. Therefore identifying the major by product which could potentially react with hydrazine and developing a strategy that isolates compound **23** from this by-product might propel the formation of the desired product **24** upon reaction with hydrazine.

[2.2.3] Third synthetic attempt

Another attempt at synthesis of compound **4** involved two steps. Step one involved the direct addition of hydrazine to the aldehyde, 4-formylbenzonitrile as shown in Scheme 12.

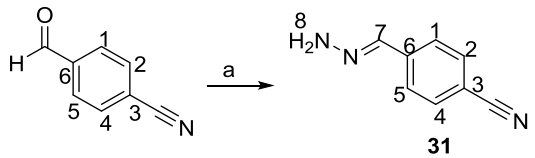

Scheme 12: Step one of third synthetic attempt. a.) NH_2NH_2, EtOH, reflux, 3 h, 80%.

This reaction produced a solid compound which was characterised. However, prior to characterising this compound, an initial examination of the structure of the desired compound **31** highlighted that ^{1}H NMR data was expected to show the presence of one set of doublets due to the equivalent H-1 and H-5 protons, another set of doublets due to the equivalent H-2 and H-4 protons, a singlet peak due to the H-7 proton and another singlet peak due the H-8 protons on the nitrogen. However, as shown in Figure 12, the ^{1}H NMR of the resultant solid from this reaction did not follow the expected pattern. Interestingly, the doublet peaks which were expected, do not show up as doublets. Instead, they show up as a singlet peak because the hydrogens in the aromatic ring are sitting on top of each other, which made the doublet peaks cancel out.

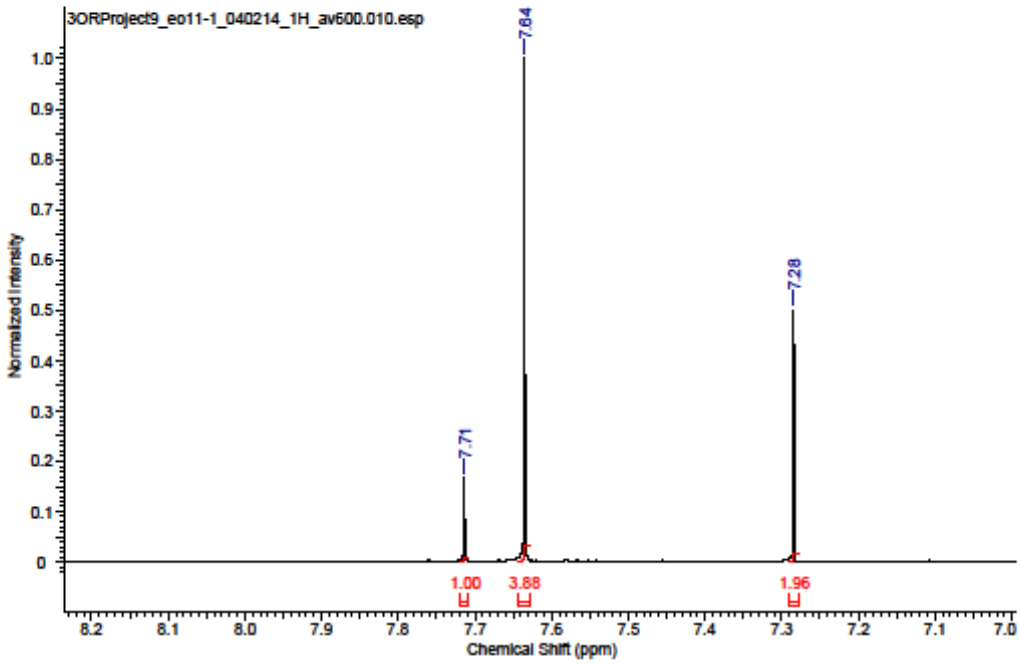

Figure 12: ^{1}H NMR of **31**

Integration of the peaks at 7.71 ppm, 7.64 ppm and 7.28 ppm revealed a 1 : 4 : 2 ratio between the H-7 proton, the four protons in the aromatic ring (H-1, H-2, H-4, H-5) and the two H-8 protons on the nitrogen. This provided evidence to suggest that the reaction had successfully worked.

The next step of this synthetic attempt was the coupling reaction of **31** and the amide product **23** as shown in Scheme 13

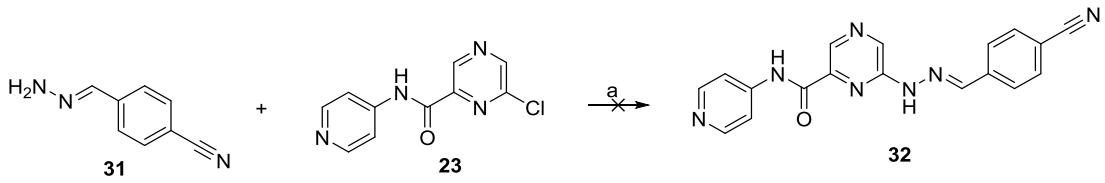

Scheme 13: Step two of third synthetic attempt. a) K_2CO_3, toluene, Pd(dppf)Cl_2, 100 °C, 2.5 h.

This reaction was done using a palladium catalyst which has been reported to work particularly well in coupling reactions involving 2-chloropyridines and hydrazine derivatives.[22] Determining the optimal condition required for this reaction was partly based on the fact that bidentate ligands are superior for the coupling of benzophenone hydrazines to chloropyridines, therefore 1,1'-bis(diphenylphosphino)ferrocene [dppf] was deemed to be the most suitable ligand. It was also determined that the undesired side product of the nucleophile was less pronounced when potassium carbonate was used, as opposed to sodium carbonate or caesium carbonate.[22] Thus, the palladium catalyst used in this experiment was the Pd(dppf)Cl_2 catalyst alongside potassium bicarbonate to form our triazolopyrazine template **32**

The next and final step of this synthetic attempt would have been the oxidative cyclisation step which had previously been carried out when trying to synthesise the triazolopyrazine core. As highlighted previously, that step proved to be very low yielding. Therefore, research into new ways of carrying out the reaction was carried out, which revealed that iodobenzene diacetate, copper(II) chloride, bromine, lead(IV) acetate and chloramine-T have been utilised for this transformation. Of these, chlormaine-T proved to be the most efficient, as it afforded rapid conversion (<2 hrs) and high yields (>85%) in most solvents.[22] If time had permitted, the next step of this synthetic route would have utilised this optimised oxidative cyclisation conditions in order to generate the triazolopyrazine core.

[3] CONCLUSION

This project provides a comprehensive overview into the techniques required and the challenges encountered when synthesising a target compound. Prospective students can develop this project further by carrying out the optimised oxidative cyclisation step described above upon which analysis of the product can provide a possible candidate for malaria testing.

[4] EXPERIMENTAL METHODS AND RAW DATA

Synthesis of triazolopyrazine core

2-chloro-6-hydrazinylpyrazine, **[6]**

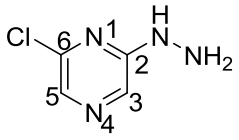

2,6-dichloropyrazine, **5** (1.123 g, 7.52 mmol) was vigorously stirred in ethanol (10 mL) and hydrazine hydrate (0.33 mL, 340 mg, 6.7 mmol) was added. The resulting mixture was heated at 105 ˚C for 16 h. After completion (monitored by TLC, 30% ethyl acetate in hexane, Rf = 0.2), the solvent was removed under vacuum to yield a crude orange solid (1.0745 g) ^{1}H NMR data derived showed significant starting material still present in the solid. Additional hydrazine (0.33 mL, 340 mg, 6.7 mmol) was added and refluxed for 20 hours at 106 ^{o}C, after which solvent was removed under vacuum to yield a crude yellow solid (0.875 g, 78%). mp: 130-132 ^{o}c. ^{1}H NMR (400 MHz, $CDCl_3$): δ 8.10 (1H, s, H-5), 7.34 (1H, s, H-3)

(E)-4-((2-(6-Chloropyrazin-2-yl)hydrazono)methyl)benzonitrile, **[7]**

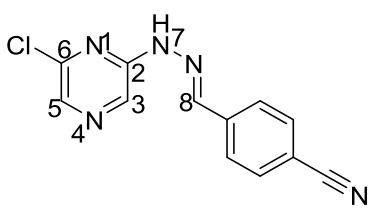

Compound **5** (0.875 g, 6.05 mmol) was stirred in acetic acid (0.41 mL) in acetonitrile (12.24 mL) and 4-formylbenzonitrile (1.10 g) was added to the orange suspension. The resulting reaction mixture was stirred at room temperature for 2 h. Solvent was removed under vacuum to yield an orange/brown solid (0.658 g, 75 %) ^{1}H NMR (400 MHz, $CDCl_3$): δ 8.69 (1H, s, H-5), 8.67 (1H, s, H-3), 8.14 (1H , s, NH), 7.97 (1H, s, H-8)

4-(5-chloro-[1,2,4]triazolo[4,3-a]pyrazin-3-yl)benzonitrile, **[10]**

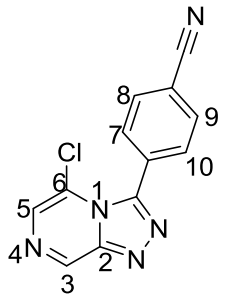

A well stirred sample of compound **7** (0.1018 g) was mixed with dichloromethane (3 mL) and phenyliodine diacetate (0.1252 g) and the mixture was stirred for 49 hours. dichloromethane (40 mL), sodium bicarbonate (40 mL) and methane (5 mL) were added to the solution. The organic extracts were then dried using magnesium sulphate and filtered, after which the solvent was removed under vacuum to yield a solid (0.014 g, 14 %) ^{1}H NMR (400 MHz, $CDCl_3$): δ 9.41 (1H, s, H-5), 7.99 (1H, s, H-3), 7.84 (4H , m, H-7, H-8, H-9, H-10)

Synthesis of substituted pyrazine ring

First attempt

2.1: Synthesis of methylpyrazine-2-carboxylate, **[17]**

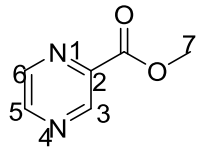

pyrazine-2-carboxylic acid, **18** (12.5 g, 100.7 mmol) was added to methanol (100 ml), and concentrated sulfuric acid (0.625 ml) was gradually added drop wise whilst stirring. The solution was refluxed at a temperature of 85^{o}c for 22 hours, then cooled to room temperature and concentrated to a volume of 25 ml. Methylenechloride (50 ml) and water (25 ml) were then added to the concentrate after which the solution was neutralised by gradual addition of saturated sodium bicarbonate (25 ml) to get a pH of approximately 8.5. An organic layer was separated and the aqueous layer was extracted again using methylenechloride (25 ml). The combined organic layers were dried over magnesium sulfate, filtered, and washed with methylenechloride (5 ml). Methylenechloride was removed under vacuum to yield a yellow solid (11.64 g, 83.7%) mp: 60^{o}C - 62^{o}C. ^{1}H NMR (300 MHz, $CDCl_3$): δ = 9.35 (d, J = 1.5 Hz, 1 H, H-5), 8.80 (d, J = 2.5 Hz, 1 H, H-6), 8.75 (dd, J3,5 = 1.5, J3,6 = 2.5 Hz, 1 H, H-3), 4.07 (s, 3 H, H-7) ppm.

2.2: methyl 4-oxy-2-pyrazinecarboxylate**, [16]**

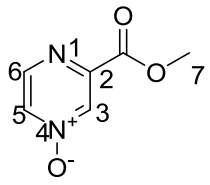

Compound **17** (5.10 g, 36.9 mmol) was suspended in 1,2 - dichloroethane (50.80 ml) and *m*CPBA (16.43 g) was added. The reaction was stirred at 60^{o}c for 18 hours, cooled to room temperature and diluted with dichloromethane (152 ml). The precipitate was filtered off and washed with additional dichloromethane (3 x 17.80 ml). The organic filtrates were combined, dried over potassium carbonate, filtered and concentrated under vacuum. The residue was suspended in hexane (25.40 ml). The product was isolated using filtration, washed with additional hexane (2 x 25.40 ml) to afford a light yellow solid (9.46 g) ^{1}H NMR showed *m*CPBA was still present. The solid was washed with addition of ethylacetate (250 ml), sodium bicarbonate (250 ml). TLC analysis (5% Et_2OAc in DCM) was carried out. Dichloromethane (250 ml) and methanol (50 ml) were added to the aqueous layer. Organic extracts were collected and concentrated under vacuum to give a solid (5.08 g, 54 %) mp:108 ^{o}c. ^{1}H NMR ($CDC1_3$, 600 MHz): 8.22 (1H, d, *J*= 2Hz, H-3 or H-5), 8.62 (1H, d, *J* = 2Hz, H-5 or H-3) 4.03 (3H, s, H-7)

methyl-6-chloro-2-pyrazinecarboxylate **[15]**

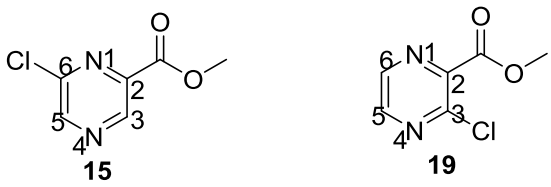

15 **19**

Compound **16** (5.08 g, 33.0 mmol) was dissolved in thionyl chloride (35.52 ml). The reaction was heated to reflux at 100^{o}C for 17 hours and allowed to cool to ambient temperature. Thionyl chloride was removed under pressure and the brown oil residue was quenched by drop wise addition of water (34.82 ml) at 0^{o}c. The mixture was then neutralized with addition of potassium carbonate (aq, 1M) and dichloromethane (5 x 69.64 ml) was added. The organic layers were collected, concentrated under vacuum to produce a brown oil residue. TLC (5% ethylacetate in dichloromethane) revealed three spots (Rf's 0.114 cm, 0.57 cm and 0.74 cm). ^{1}H NMR (600 MHz, $CDCl_3$): δ = 9.23 (s, 1 H, H-3 or H-5), 8.82 (s, 1 H, H-3 or H-5)

The oil was purified by silica gel chromatography (5% ethyl acetate in dichloromethane) Three spots were produced (Rf's 0.586, 0.594, 0.125) and the solutions were collected corresponding to each spot. The solvents were removed under vacuum and ^{1}H NMR was derived for each corresponding solid.

First eluted sample (1.11 g, 22%) mp: 40 – 43^{o}c, ^{1}H NMR (600 MHz, $CDCl_3$): δ = 9.23 (s, 1 H, H-3 of H-5), 8.82 (s, 1 H, H-3 or H-5),

Second eluted sample (2.30 g, 45%) mp: 65^{o}c ^{1}H NMR (600 MHz, $CDCl_3$): δ = 9.54 (s, 1 H,), 8.54 (s, 1 H,)

Third eluted sample, **19** (1.05 g, 21%) mp: 35^{o}c ^{1}H NMR (600 MHz, $CDCl_3$): δ = 9.35 (d, 1 H, J = 1.5 MHz, H-5), 8.80 (d, 1 H, J =1.5 MHz, H-6)

6-chloropyrazine-2-carboxylic acid, **[14]**

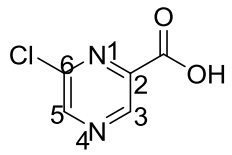

m/z: 157.99 (100.0%), 159.99 (32.4%),
158.99 (6.3%), 160.99 (1.8%)

The solid from the first eluted solution of **15** (0.90 g, 5.68 mmol) was dissolved in ethanol (12.64 mL) and sodium hydroxide (2M, 12.64 ml) was added. The reaction mixture was stirred at ambient temperature for 2 hours then acidified to pH3 with hydrochloric acid (2M). The mixture was then diluted with water (75.84 mL) and extracted with ethyl acetate (4 x 50.56 mL). The organic extracts were combined, washed with brine (50.56 ml), dried over magnesium sulfate, filtered and concentrated under vacuum to provide a white solid (0.44 g, 49 %). ^{1}H NMR (DMSO-d_6, 500 MHz) δ 9.18 (s, 1H, H-3 or H-5). 9.07 (s, 1H, H-5 or H-3), MS (157.9, M^+)

6-hydrazinepyrazine-2-carboxylic acid, **[13]**

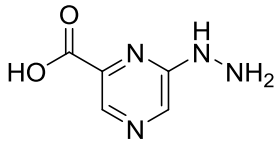

m/z: 154.05 (100.0%), 155.05 (7.0%)

Compound, **14** (0.029 g, 0.182 mmol) was vigorously stirred in ethanol (0.52 mL) and hydrazine hydrate (0.0132 mL) was added. The resulting mixture was sealed in a tube and heated at 78°C for 16 h. After completion, the solvent was removed under vacuum to yield an orange solid (0.018 g, 62%). MS: 169.0 (M^+ + $NHNH_2$) Mass spectrum data inconsistent with expected data so unsuccessful synthesis

Second Attempt

6-chloro-N-(pyridin-4-yl)pyrazine-2-carboxamide, **[23]**

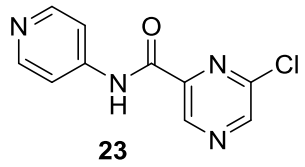

23

m/z: 234.03 (100.0%), 236.03 (32.1%), 235.03 (12.3%), 237.03 (3.5%)

Compound **14** (0.1 g, 0.63 mmol) in dimethylformamie (5 ml) was added to EDC (0.108 g), HOBt (0.1063 g) and stirred for 30 minutes. 4- aminopyridine (0.065 g) was then added, followed by DIPEA (0.23 ml). The reaction was stirred for 22 hours, after which it was diluted with water. The resultant solution was dried under vacuum to provide the liquid (1.3 ml). Hydrochloric acid (0.1 M, 1.3 ml) and ethyl acetate (5 ml) were added to the liquid. The organic layer was washed with 5% lithium chloride(aq) (4 x 3 ml). The combined organic extracts were concentrated under vacuum to give the solid product (0.025 g, 25%) MS: 234.0 (M^+) ^{1}H NMR (600 MHz, $CDCl_3$): δ = 7.954 (s, 1 H, NH)

6-hydrazinyl-N-(pyridin-4-yl)pyrazine-2-carboxamide, **[24]**

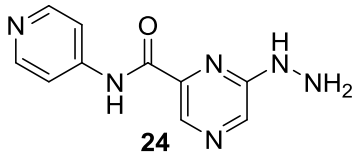

24

m/z: 230.09 (100.0%), 231.09 (13.0%)

Compound **23** (0.025 g) was vigorously stirred in ethanol (10 mL) and hydrazine hydrate (0.33 mL) was added. The resulting mixture was heated at 105˚C for 60 hrs. After completion, the solvent was removed under vacuum to yield a crude orange liquid. Hydrochloric acid (0.1 M, 0.9 ml) and ethyl acetate (5 ml) were

added to the liquid. The organic layer was washed with 5% lithium chloride (aq, 4 x 3 ml). The combined organic extracts was concentrated under vacuum to give the solid product (0.015 g, 60%) MS: 159.0. Mass spectrum data inconsistent with expected data so unsuccessful synthesis

Third synthetic attempt

4- hydrazonebenzonitrile, **[31]**

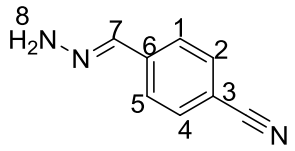

4-formylbenzonitrile (1.31 g) was added to a solution of 100% hydrazine hydrate (4.9 ml) in ethanol (10 ml). The reaction was refluxed for 3 hrs at 105^{o}C and cooled to room temperature. No precipitate was produced, the ethanol was removed under vacuum to yield a yellow liquid (5.18 g) Ethanol (8 ml) was added to the liquid and concentrated under vacuum to produce yellow crystals. (1.05 g, 80%) mp: 48^{0}c-50^{o}c. 1H NMR (600 MHz, $CDCl_3$): δ = 7.71 (s, 1 H, H-7) 7.64 (s, 4H, H-1, H-2, H-4, H-5) 7.28 (s, 2H, H-8)

6-[(2E)-2-(4-cyanobenzylidene)hydrazinyl]-N-(pyridin-4-yl)pyrazine-2-carboxamide, **[32]**

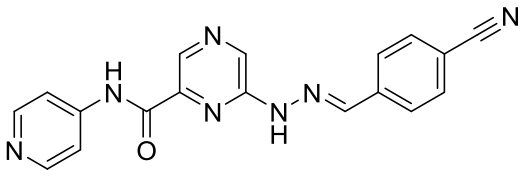

m/z: 343.12 (100.0%), 344.12 (22.2%), 345.12 (2.5%)

A three necked round bottomed flask was fitted with a reflux condenser and two stoppers. Compound **23** (0.1547 g) was added to the flask. Potassium carbonate (0.2209 g) was also added and the flask was flushed with nitrogen. Toluene (1.238 ml) and 4-hydrazonebenzonitrile, **31** (0.25 g) were added, followed by Pd(dppf)CL_2. (0.0040 g). The flask was flushed again with nitrogen and the reaction mixture was heated to 100^{o}c for 2.5 hours. The reaction mixture was then cooled to room temperature and water (0.572 ml) was added. The mixture was stirred at room temperature for 15 minutes and then filtered through a filter funnel. The resulting wet cake solid was rinsed with toluene (3 x 0.286 ml) and air dried to give the solid (0.04g, 25 %) MS: 254.5 Mass spectrum data inconsistent with expected data so unsuccessful synthesis

[5] REFERENCES

1) Mcnamara, D. T.; Kasehagen, L. J.; Grimberg, B. T.; Cole-Tobian , J.; Collins, W. E.; Zimmerman, P. A. *The American Journal of Tropical Medicine and Hygiene*. **2006**, *74*, 413–421.

2) World Health Organization Website, ***www.who.int/mediacentre/factsheets/fs094/en/,*** Date accessed: **07/02/2014**.

3.) Newman, R. D.; Parise, M. E.; Barber, A. M.; Steketee, R. W. *Annals of Internal Medicine*. **2004**, *141*, 547-555.

4.) White, N. J. *The Journal of Clinical Investigation.* **2004,** *113*, 1084–1092.

5.) White, N. J. *Antimicrobial agents and chemotherapy.* **1997**, *41*, 1413-1422.

6.) Foley, M.; Tilley, L. *Pharmacology & Therapeutics*. **1998**, *79*, 55–87.

7.) Hall, N.; Kerras, M.; Raine , J. D.; Carlton, J. M.; Kooij , T. W. A.; Berriman, M.; Florens, L.; Janssen, C. S.; Pain, A.; Christophides , G. K.; James, K.; Rutherford, K.; Harris, B.; Harris, D.; Churcher, C.; Quail, M. A.; Ormond, D.; Doggett, J.; Trueman, H. E.; Mendoza, J.; Bidwell, S. L.; Rajandream, M.; Carucci, D. J.; Yates III, J. R.; Kafatos, F. C.; Janse, C. J.; Barrell, B.; Turner, C. M. R.; Waters, A. P.; Sinden, R. E. *Science*. **2005**, *307*, 82-86.

8.) Open Source Malaria Webpage ***http://malaria.ourexperiment.org/data/7353.html,*** Date accessed: **02/ 02/ 2014.**

9.) Krishna, S.; Woodrow, C.; Webb, R.; Penny, J.; Takeyasu, K.; Kimura, M.; East, J. M. *Journal of Biological Chemistry*. **2001**, *276*, 10782-10787.

10.) Bradac, J.; Furek, Z.; Janezic, D.; Molan, S.; Smerkolj, I.; Stanovnik, B.; Tisler, M.; Vercek, B. *The Journal of Organic Chemistry.* **1977**, *42*, 4197 – 4201.

11.) Yu, W.; Du, Y.; Zhao, K. *Organic Letters*. **2009**, *11*, 2417-2420.

12.) Open Source Malaria Online Lab Notebook ***http://malaria.ourexperiment.org/triazolopyrazine_se/byuser/www.google.com-accounts-o8-id id=AItOawmEjK3bt7yI4QzJmveCLN2gxtJpm9NpHqk/page/10,*** Date accessed: **10/03/2014**

13.) Hellyer, R. M.; Larsen, D. S.; Brooker, S. *European Journal of Inorganic Chemistry*. **2009**, *2009*, 1162–1171.

14.) Seizaburo, O.; Akira, K.; Tsuneo, K.; Fumihiko, U. *Chemical and Pharmaceutical Bulletin.* **1971**, *19*, 1344-1357.

15.) Kin-Ihi, L.; Mitsuhiko, M.; Takuji S.; Toshimi M. *Chemical and Pharmaceutical Bulletin.* **1981,** *29*, 88-97.

16) Clayden, J.; Greeves, N.; Warren, S. *Organic Chemistry.* 2nd Edition, 730.

17.) Scanio, M. J. C.; Shi, L.; Bunnelle, W. H.; Anderson, D. J.; Helfrich, R. J.; Malysz, J.; Thorin-Hagene, K. K.; Van Handel, C. E.; Marsh, K. C.; Lee, C.; Gopalakrishnan, M. *Journal of Medicinal Chemistry*. **2011**, *54*, 7678–7692.

18) Clayden, J.; Greeves, N.; Warren, S. *Organic Chemistry.* 2nd Edition, 726.

19) So-Yeop, H.; Young-Ah, K. *Tetrahedron.* **2004,** *60,* 2447–2467.

20) Naoki, N.; Yoshito, I. *Bioconjugate Chemistry***. 1995,** *6*, 123-130.

21) Desai, M. C.; Stephens Stramiello, L. M. *Tetrahedron Letters.* **1993,** *34*, 7685–7688.

22.) Thiel, O. R.; Achmatowicz, M. M.; Reichelt, A.; & Larsen, R. D. *Angewandte Chemie*. **2010**, *122*, 8573-8576.